J Fluoresc (2012) 22:253–259
DOI 10.1007/s10895-011-0955-7

ORIGINAL PAPER

A Pyrene-based Highly Selective Turn-on Fluorescent Sensor for Copper(II) Ion and its Application in Live Cell Imaging

Shu-Pao Wu · Zhen-Ming Huang · Shi-Rong Liu · Peter Kun Chung

Received: 20 June 2011 / Accepted: 10 August 2011 / Published online: 26 August 2011
© Springer Science+Business Media, LLC 2011

Abstract A new pyrene derivative (chemosensor **1**) containing a picolinohydrazide moiety exhibits high selectivity for Cu^{2+} ion detection in mixed aqueous media ($CH_3OH:H_2O$= 7:3). Significant fluorescence enhancement was observed with chemosensor **1** in the presence of Cu^{2+}. However, the metal ions Ag^{+}, Ca^{2+}, Cd^{2+}, Co^{2+}, Cu^{2+}, Fe^{2+}, Fe^{3+}, Hg^{2+}, K^{+}, Mg^{2+}, Mn^{2+}, Ni^{2+}, Pb^{2+}, and Zn^{2+} produced only minor changes in fluorescence for the system. The apparent association constant (K_a) of Cu^{2+} binding in chemosensor **1** was found to be $2.75*10^3$ M^{-1}. The maximum fluorescence enhancement caused by Cu^{2+} binding in chemosensor **1** was observed over the pH range 5–8. Moreover, by means of fluorescence microscopy experiments, it is demonstrated that **1** can be used as a fluorescent probe for detecting Cu^{2+} in living cells.

Keywords Cu^{2+} · Fluorescence · Chemosensor · Pyrene · Live cell imaging

Introduction

Copper, after iron and zinc, is the third most abundant essential transition metal ion in the human body and plays important roles in various biological processes. Many proteins contain copper ions as part of a catalytic center. Free copper ions in a live cell catalyze the formation of reactive oxygen species (ROS) that can damage lipids, nucleic acids, and proteins. Research has connected the cellular toxicity of copper ions with serious diseases including Alzheimer's disease [1], Indian childhood cirrhosis (ICC) [2], prion disease [3], and Menkes and Wilson diseases [4, 5]. Due to its extensive applications, the copper ion is also a significant metal pollutant. The limit of copper in drinking water set by the US Environmental Protection Agency (EPA) is 1.3 ppm (~20 μM). Numerous methods for the detection of copper ions in a sample have been proposed, including atomic absorption spectrometry [6], inductively coupled plasma mass spectroscopy (ICPMS) [7], inductively coupled plasma-atomic emission spectrometry (ICP-AES) [8], and voltametry [9]. Most of these methods cannot be used for assays because they entail the destruction of the sample. Consequently, more attention is being focused on the development of fluorescent chemosensors for the detection of Cu^{2+} ions [10–24].

Developing metal ion fluorescent chemosensors usually involves combining a metal-binding unit with a fluorophore. The presence of metal ions is signaled, during interaction with binding units, by changes in emission intensity or wavelength. Because Cu^{2+} is known as a fluorescence quencher, most fluorescent chemosensors detect Cu^{2+} through a fluorescence-quenching process that undergoes a charge or energy transfer mechanism [20]. However, fluorescent chemosensors using fluorescence enhancement are more sensitive to metal ions than are those using fluorescence quenching. This paper reports on a newly designed pyrene-based fluorescent enhancement chemosensor for Cu^{2+} based on photoinduced electron transfer (PET). Binding Cu^{2+} to the chemosensor blocks PET and greatly enhances fluorescence of pyrene.

In this study, a pyrene-based fluorescent chemosensor was designed for metal ion detection. Two parts make up chemosensor **1**: a pyrene moiety as a reporter and a picolinohydrazide as a chelator for the metal ion. Chemosensor **1** was synthesized through the reaction of 1-pyrenecarboxaldehyde hydrazone and picolinyl chloride (Scheme 1). Chemosensor **1** exhibits weak fluorescence due to fluorescence quenching by photoinduced electron transfer from the lone pair of electrons

S.-P. Wu (✉) · Z.-M. Huang · S.-R. Liu · P. K. Chung
Department of Applied Chemistry,
National Chiao Tung University,
Hsinchu, Taiwan 300, Republic of China
e-mail: spwu@mail.nctu.edu.tw

Scheme 1 The synthesis of chemosensor **1**

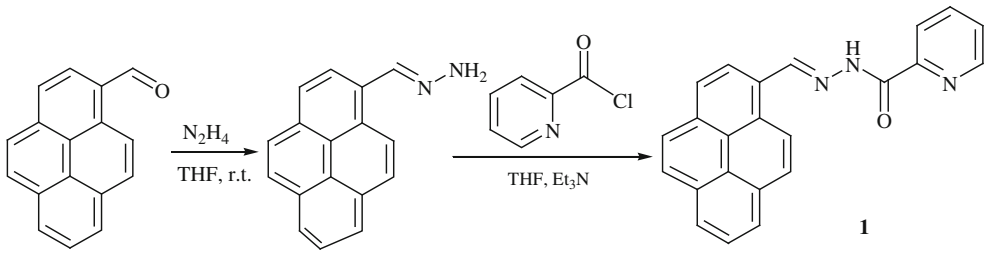

on the nitrogen atom to pyrene. Binding metal ions to the chemosensor blocks PET and greatly enhances fluorescence of pyrene. The metal ions Ag^{+}, Ca^{2+}, Cd^{2+}, Co^{2+}, Cu^{2+}, Fe^{2+}, Fe^{3+}, Hg^{2+}, K^{+}, Mg^{2+}, Mn^{2+}, Ni^{2+}, Pb^{2+}, and Zn^{2+} were tested for metal ion binding selectivity with chemosensor **1**, but Cu^{2+} was the only ion that caused a blue emission upon binding with chemosensor **1**. The fluorescence microscopy experiments also demonstrated that **1** can be used as a fluorescent probe for detecting Cu^{2+} in living cells.

Experimental Section

Materials and Instrumentations

All solvents and reagents were obtained from commercial sources and used as received without further purification. UV/Vis spectra were recoreded on an Agilent 8453 UV/Vis spectrometer. IR data were obtained on Bomem DA8.3 Fourier-Transform Infrared Spectrometer. NMR spectra were obtained on a Bruker DRX-300 NMR spectrometer. Fluorescence imagings were obtained on a ZEISS Axio Scope A1 Fluorescence Microscope.

Synthesis of [*N*′-(pyren-3-yl)methylene]picolinohydrazide (chemosensor **1**)

The reaction mixture containing picolinic acid (135.42 mg, 1.1 mmol) and thionyl chloride (0.146 ml, **2**mmol) in 10 mL of CH_3CN was reflux for one hour. The solvent was removed by rotor vacuum, and THF was added to dissolve the product (picolinoyl chloride). 1-Pyrenecarboxaldehyde hydrazone (244 mg, 1 mmol) and triethylamine (0.418 ml, 3 mmol) were added to the previous solution containing picolinyl chloride. The reaction mixture was stirred at room temperature for four hours. Thereafter, the solvent was evaporated under reduced pressure, and the crude product was purified by column chromatography (hexane/dichloromethane/ethyl acetate=2:1:1) to give chemosensor **1** as a pale yellow solid. Yield: 47%; mp, 252 °C. EI-Mass m/z (%), 349 (16.12%), 227 (100%), 213 (24.68%); HR-MS (EI) calcd for $C_{23}H_{15}O_1N_3$ $[M]^{+}$ 349.1215; found 349.1208. ^{1}H NMR (300 MHz, $CDCl_3$): δ 11.25 (1H, s) , 9.37 (1H, s), 8.77 (2H, d, *J*=7.8 Hz), 8.65 (1H, d, *J*=4.8 Hz), 8.38 (1H, d, *J*=7.8 Hz), 8.22 (4H, m), 8.12 (1H, t, *J*=7.8 Hz), 8.04 (1H, t, *J*=7.8 Hz), 7.94 (1H, td, *J*=1.8, 7.8 Hz), 7.50–7.55 (1H, m). ^{13}C NMR (75 MHz, $CDCl_3$) δ 160.5, 149.6, 148.5, 147.6, 138.1, 133.3, 131.7, 131.0, 129.9, 129.3, 129.0, 127.9, 127.2, 126.7, 126.6, 126.4, 126.2, 126.1, 125.5, 125.2, 125.0, 123.4, 122.6. IR (KBr) 3462 (NH), 1667 (C=O), 1587 (C=C, C=N) cm^{-1}.

Metal Ion Binding Study by UV-vis and Fluorescence Spectroscopy

Chemosensor **1** (25 μM) was added with different metal ions (50 μM). All spectra were measured in 1.0 mL methaol-water solution (v/v=7/3, 6 mM Hepes buffer, pH 7.0). The light path length of cuvvet was 1.0 cm.

The pH Dependence on Cu^{2+} Binding in Chemosensor **1** Studied by Fluorescence Spectroscopy

Chemosensor **1** (25 μM) was added with Cu^{2+} (100 μM) in 1.0 mL methaol-water solution (v/v=7/3, 6 mM buffer). The buffers were: pH 1 ~2, KCl/HCl; pH 2.5~4, KH_2PO_4/HCl; pH 4.5~6, KH_2PO_4/NaOH; pH 6.5~10 Hepes.

Determination of the Binding Stochiometry and the Apparent Association Constants K_a of Cu(II) Binding in Chemosensor **1**

The binding stochiometry of **1**-Cu^{2+} complexes was determined by Job plot experiments [25]. The fluorescence intensity at 455 nm was plotted against molar fraction of **1** under a constant total concentration. The total concentration of sensor and Cu^{2+} ion was 25 μM. When the emission intensity reaches a maximum point, the molar fraction represents the binding stochiometry of **1**-Cu^{2+} complexes. In Fig. 4, maximum emission intensity was reached when the molar fraction was 0.5. These results indicate that chemosensor **1** forms a 1:1 complex with Cu^{2+}. The apparent association constants (K_a) of **1**-Cu^{2+} complexes was determined by the Benesi-Hildebrand Eq. 1 [26, 27]:

$$1/(F - F_0) = 1/\{K_a{}^{*}(F_{max} - F_0){}^{*}[Cu^{2+}]\} + 1/(F_{max} - F_0) \quad (1)$$

, where F is the fluorescence intensity at 455 nm at any given Cu^{2+} concentration, F_0 is the fluorescence intensity

at 455 nm in the absence of Cu^{2+}, and F_{max} is the maxima fluorescence intensity at 455 nm in the presence of Cu^{2+} in solution. The association constant K_a was evaluated graphically by plotting $1/(F\text{-}F_0)$ against $1/[Cu^{2+}]$. Typical plots ($1/(F\text{-}F_0)$ *vs.* $1/[Cu^{2+}]$) are shown in Fig. 5. Data were linearly fitted according to Eq. 1 and the K_a value was obtained from the slope and intercept of the line.

Cell Culture

The cell line HeLa was provided by the Food Industry Research and Development Institute (Taiwan). The HeLa cells were grown in DMEM (Dulbecco's modified Eagle's medium) supplemented with 10% FBS (fetal bovine serum) at 37 °C and 5% CO_2. Cells were plated on 14 mm glass coverslips and allowed to adhere for 24 h.

Fluorescence Imaging

Experiments to assess Cu^{2+} uptake were performed in PBS with 10 μM $CuCl_2$. Treat the cells with 2 μL of 10 mM metal ions (final concentration: 10 μM) dissolved in sterilized PBS (pH 7.4) and incubate for 0.5–1 h at 37 °C.Wash the treated cells three times with 2 mL PBS to remove the remaining metal ions. Add 2 mL culture media to the cell culture and treat the cell culture with 2 μL of 10 mM chemosensor **1** (final concentration: 10 μM) dissolved in DMSO. Incubate for 30 min at 37 °C. Remove culture media and wash the treated cells three times with 2 mL PBS before observation. Fluorescence imaging was performed with a ZEISS Axio Scope A1 Fluorescence Microscope. Cells loaded with **1** were excited at 350 nm using a lamp (Hg 50 W). Emission was collected at 460 nm.

Results and Discussion

Spectral Characteristics of Chemosensor 1

The synthesis of chemosensor **1** consisted of two steps (scheme 1): the formation of 1-pyrenecarboxaldehyde hydrazone and its further reaction with picolinoyl chloride. Chemosensor **1** is colorless and has an absorption band centered at 360 nm, which is near the typical absorption band of pyrene, 335 nm [28]. In addition, chemosensor **1** exhibits weaker fluorescence (Φ=0.013) than does pyrene (Φ= 0.6~0.9) [29]. This is due to fluorescence quenching by PET from the lone pair of electrons on the nitrogen atom to pyrene.

Cation-sensing Properties

The sensing ability of chemosensor **1** was tested by mixing it with the metal ions Ag^{+}, Ca^{2+}, Cd^{2+}, Co^{2+}, Cu^{2+}, Fe^{2+}, Fe^{3+}, Hg^{2+}, K^{+}, Mg^{2+}, Mn^{2+}, Ni^{2+}, Pb^{2+}, and Zn^{2+}. To further evaluate the selectivity of chemosensor **1** toward various metal ions, the fluorescence spectra of chemosensor **1** were taken in the presence of several transition metal ions. Cu^{2+} was the only metal ion that caused a significant blue emission (Fig. 1). During Cu^{2+} titration with chemosensor **1**, a new emission band centered at 455 nm formed (Fig. 2). After adding two equivalents of Cu^{2+}, the emission

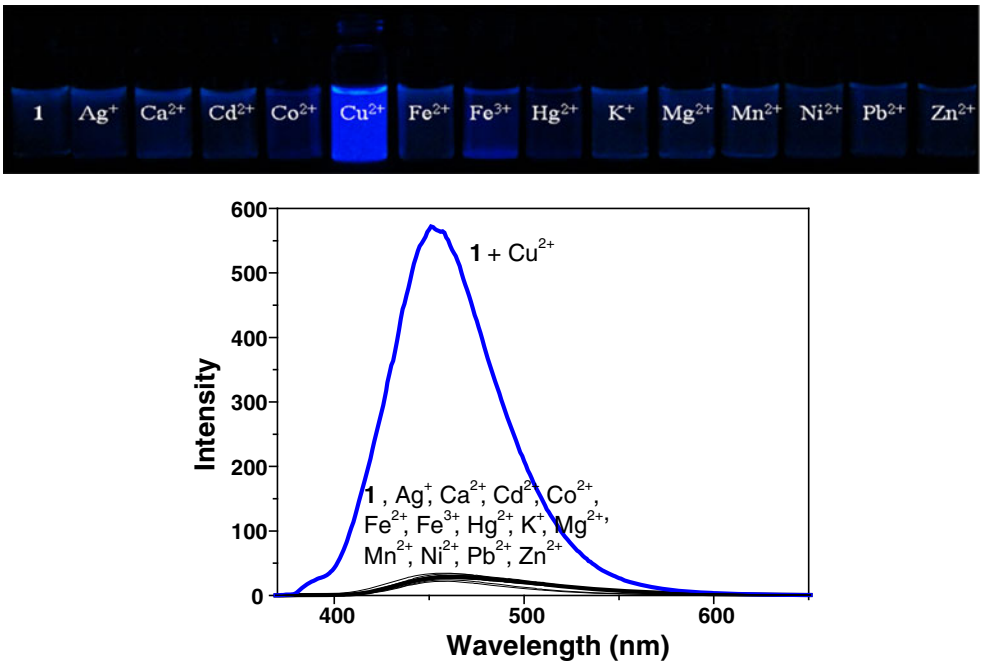

Fig. 1 Fluorescence emission (*top*) and spectra (*bottom*) of chemosensor **1** (25 μM) upon addition of various metal ions (50 μM) in methanol-water (v/v=7:3, 6 mM HEPES, pH 7.0) solutions. The excitation wavelength was 360 nm

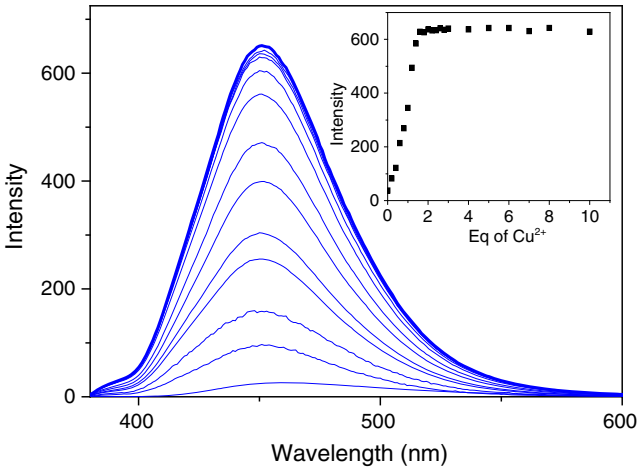

Fig. 2 Fluorescence response of chemosensor **1** (25 μM) to various equivalents of Cu^{2+} in methanol-water (v/v=7:3, 6 mM HEPES, pH 7.0) solutions. The excitation wavelength was 360 nm

intensity reached a maximum. The quantum yield of that emission band was 0.267, which is 20-fold that of chemosensor **1,** 0.013. These observations indicate that Cu^{2+} is the only metal ion that readily binds with chemosensor **1**, significantly enhancing fluorescence and permitting highly selective detection of Cu^{2+}.

To study the influence of other metal ions on Cu^{2+} binding with chemosensor **1**, this research tested Cu^{2+} (100 μM) in combination with each of the other metal ions (100 μM) (Fig. 3). Fluorescence enhancement caused by the mixture of Cu^{2+} with most metal ions was similar to that caused by Cu^{2+} alone. This observation indicates that most of the other metal ions did not interfere with the binding of chemosensor **1** with Cu^{2+}.

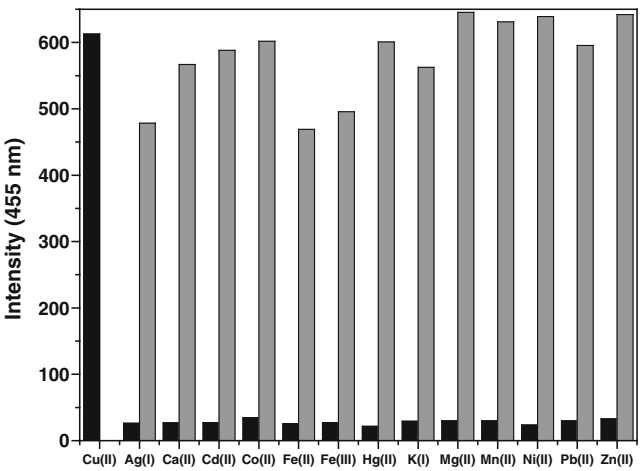

Fig. 3 Fluorescence response of chemosensor **1** (25 μM) to Cu^{2+} (100 μM) or 100 μM of other metal ions (*black bars*) and to the mixture of the other metal ions (100 μM) with 100 μM of Cu^{2+} (*gray bar* portions) in methanol-water (v/v=7:3, 6 mM HEPES, pH 7.0) solutions

Stoichiometries and Affinity Constants of **1**-Cu^{2+} Complexes

In order to understand the binding stochiometry of chemosensor **1**-Cu^{2+} complexes, Job plot experiments were carried out. Figure 4 plots the emission intensity at 455 nm against molar fraction of chemosensor **1** given a constant total concentration. Maximum emission intensity was reached when the molar fraction was 0.5, corresponding to a 1:1 ratio between chemosensor **1** and Cu^{2+}. This binding ratio (1:1) for **1**-Cu^{2+} complexes was also supported by ESI Mass in which a peak at 412 (m/z) represents the formation of a 1:1 complex. The association constant K_a was evaluated graphically by plotting $1/\Delta F$ against $1/[Cu^{2+}]$ (Fig. 5). The data were linearly fit according to the Benesi–Hilderbrand equation. The K_a value, obtained from the slope and intercept of the line, was found to be $2.75*10^3$ M^{-1}.

To gain a clearer understanding of the structure of chemosensor **1**-Cu^{2+} complexes, ^1H NMR and Infrared (IR) spectroscopy were employed. Cu^{2+} is a paramagnetic ion and can affect the proton signals that are close to a Cu^{2+} binding site. In the ^1H NMR spectra of chemosensor **1**, adding Cu^{2+} caused the proton (amide NH) signal at 12.4 ppm to almost completely disappear (Fig. 6), the proton (at pyridine) signals at 7.6 and 8.8 ppm to disappear, and the intensity of the proton (CH=N) signal at 9.8 ppm to decrease. Other peaks (protons at pyrene) remained unchanged. These observations indicated the binding of Cu^{2+} with an amide group and pyridine. The IR spectra were primarily characterized by bands in the double-bond region. The band 1660 cm^{-1} was associated with double-bond (C=O and C=N) absorption in chemosensor **1**. Binding of Cu^{2+} with chemosensor **1** resulted in a new broad band at 1633 cm^{-1} in the double-bond absorption region, due to the amide group in chemosensor **1**.

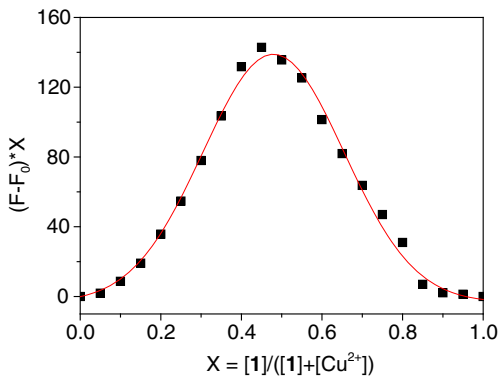

Fig. 4 Job plot of the chemosensor **1**-Cu^{2+} complexes in methanol-water (v/v=7:3, 6 mM HEPES, pH 7.0) solutions. The total concentration ([chemosensor **1**] + [Cu^{2+}]) was 25 μM

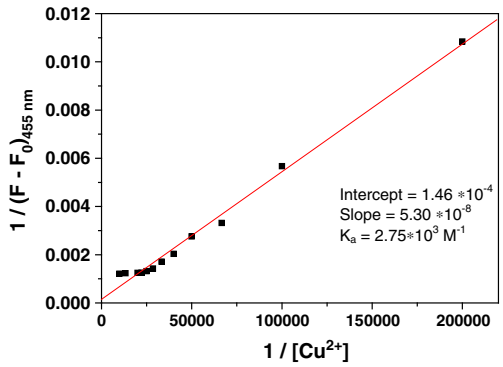

Fig. 5 Benesi-Hildebrand plot of the chemosensor **1**-Cu^{2+} complexes in methanol-water (v/v=7:3, 6 mM HEPES, pH 7.0) solutions

The Job plot indicates that the binding ratio for chemosensor **1**-Cu^{2+} complexes was 1:1. Cu^{2+} was bound to one nitrogen atom from pyridine and one nitrogen atom from amide (Fig. 7).

The study performed pH titration of chemosensor **1** to investigate a suitable pH range for Cu^{2+} sensing. As depicted in Fig. 8, the emission intensities of metal-free chemosensor **1** were very low. When pH fell below 2, the emission intensity increased, due to the protonation on the amine in the imine bond. After mixing chemosensor **1** with Cu^{2+}, the emission intensity at 455 nm increased and reached maximum in the pH range of 6–8. Above pH 8.0, the emission intensity decreased. This indicates poor stability of the chemosensor **1**-Cu^{2+} complexes at high pH values. At pH<4, the emission intensity decreased, due to the protonation of the amine groups that prevented the formation of chemosensor **1**-Cu^{2+} complexes.

Live Cell Imaging

Chemosensor **1** was further applied for live cell imaging. For the detection of Cu^{2+} in live cells, HeLa cells were

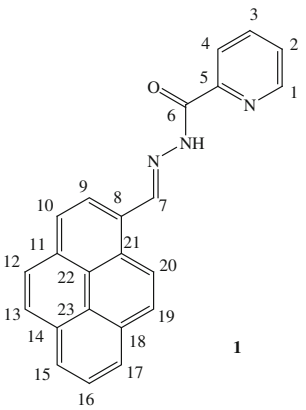

1

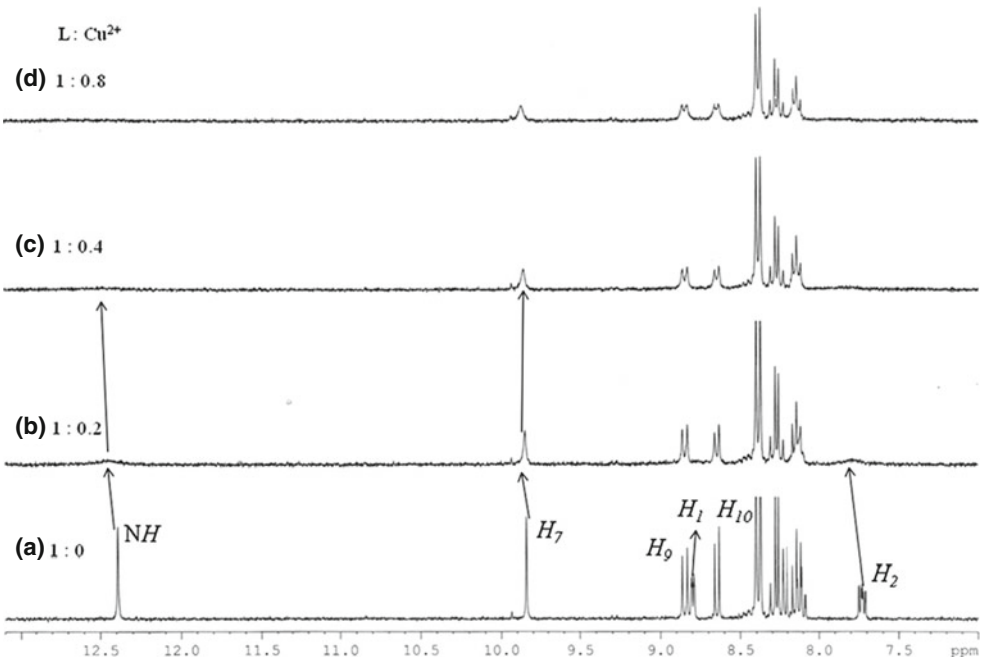

Fig. 6 ^1H NMR spectra of Chemosensor **1** (5 mM) in the presence of different amount of Cu^{2+} in DMSO-d_6

Fig. 7 A proposed 1:1 complex formed between chemosensor **1** and Cu^{2+}

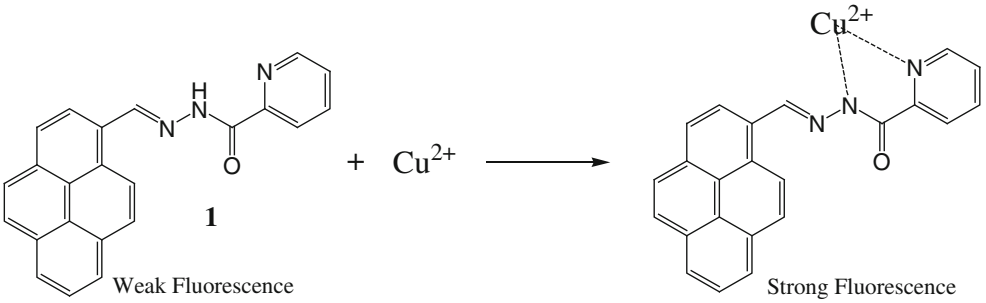

cultured in DMEM supplemented with 10% FBS at 37 °C and 5% CO_2. Cells were plated on 14 mm glass coverslips and allowed to adhere for 24 h. HeLa cells were treated with 10 μM $CuCl_2$ for 1 h and washed with PBS for three times. Then cells were incubated with chemosensor **1** (10 μM) for 30 min and washed with PBS to remove the remaining sensor. The images of the HeLa cells were obtained by a fluorescence microscope. Figure 9 shows the images of HeLa cells with chemosensor **1** after the treatment of Cu^{2+}. The overlay of fluorescence and bright-field images reveals that the fluorescence signals are localized in the intracellular area, indicating a subcellular distribution of Cu^{2+} and good cell-membrane permeability of chemosensor **1**.

Conclusion

This study developed a pyrene-based fluorescent chemosensor for Cu^{2+} sensing. The experiment synthesized chemosensor **1** from the reaction of 1-pyrenecarboxaldehyde hydrazone and picolinoyl chloride to form an amide bond. Fluorescence was significantly enhanced with chemosensor **1** in the presence of Cu^{2+}, but adding instead Ag^{+}, Ca^{2+}, Cd^{2+}, Co^{2+}, Fe^{2+}, Fe^{3+}, Hg^{2+}, K^{+}, Mg^{2+}, Mn^{2+}, Ni^{2+}, Pb^{2+}, or Zn^{2+} to the chemosensor solution barely affected fluorescence emission. The optimal pH range for Cu^{2+} detection by chemosensor **1** is 5~8. This pyrene-based Cu^{2+} chemosensor also provides an effective method of Cu^{2+} sensing in live cell imaging.

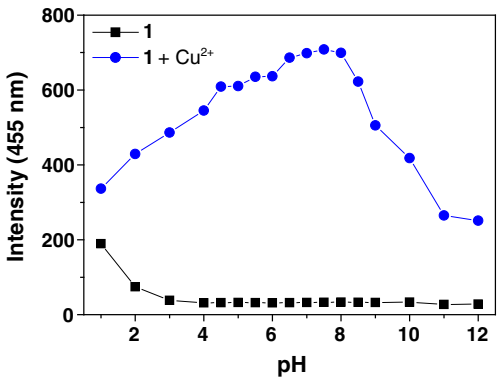

Fig. 8 Fluorescence intensity (455 nm) of free chemosensor **1** (25 μM)(*black squares*) and after addition of Cu^{2+} (100 μM) (*blue circles*) in methanol-water (v/v=7:3, 6 mM beffer) solutions as a function of pH. The excitation wavelength was 360 nm

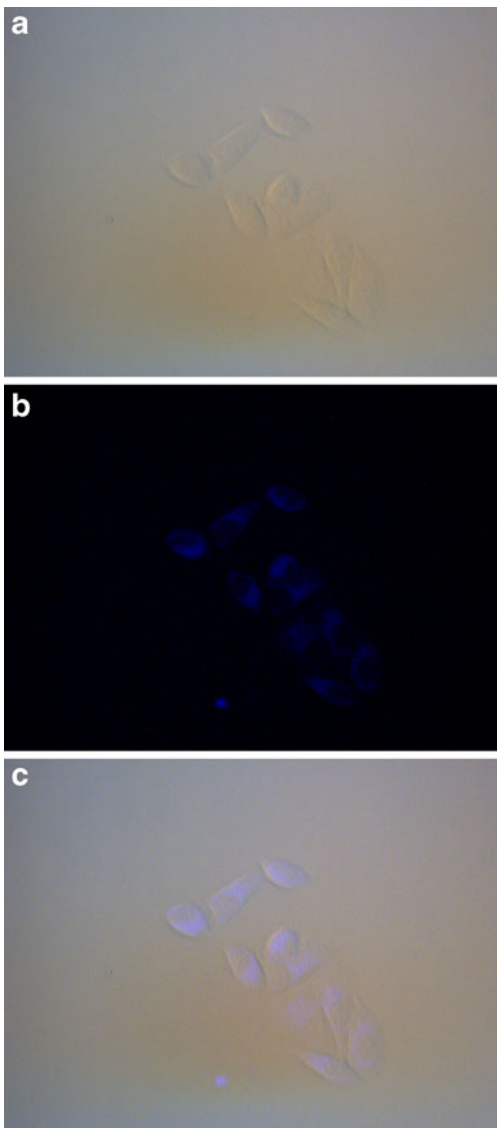

Fig. 9 Cu^{2+}-treated HeLa cell images. **a** bright field image; **b** fluorescence image; **c** merged image

Acknowledgments We gratefully acknowledge the financial supports of the National Science Council (ROC) and National Chiao Tung University.

References

1. Bull PC, Thomas GR, Rommens JM, Forbes JR, Cox DW (1993) The Wilson disease gene is a putative copper transporting P-type ATPase similar to the Menkes gene. Nat Genet 5:327–337
2. Hahn SH, Tanner MS, Danke DM, Gahl WA (1995) Normal metallothionein synthesis in fibroblasts obtained from children with indian childhood cirrhosis or copper-associated childhood cirrhosis. Biochem Mol Med 54:142–145
3. Barnham KJ, Masters CL, Bush AI (2004) Neurodegenerative diseases and oxidatives stress. Nat Rev Drug Discov 3:205–214
4. Waggoner DJ, Bartnikas TB, Gitlin JD (1999) The role of copper in neurodegenerative disease. Neurobiol Disease 6:221–230
5. Vulpe C, Levinson B, Whitney S, Packman S, Gitschier J (1993) Isolation of a candidate gene for Menkes disease and evidence that it encodes a copper-transporting ATPase. Nat Genet 3:7–13
6. Gonzales APS, Firmino MA, Nomura CS, Rocha FRP, Oliveira PV, Gaubeur I (2009) Peat as a natural solid-phase for copper preconcentration and determination in a multicommuted flow system coupled to flame atomic absorption spectrometry. Anal Chim Acta 636:198–204
7. Becker JS, Matusch A, Depboylu C, Dobrowolska J, Zoriy MV (2007) Quantitative imaging of selenium, copper, and zinc in thin sections of biological tissues (slugs-genus arion) measured by laser ablation inductively coupled plasma mass spectrometry. Anal Chem 79:6074–6080
8. Liu Y, Liang P, Guo L (2005) Nanometer titanium dioxide immobilized on silica gel as sorbent for preconcentration of metal ions prior to their determination by inductively coupled plasma atomic emission spectrometry. Talanta 68:25–30
9. Ensafi AA, Khayamian T, Benvidi A (2006) Simultaneous determination of copper, lead and cadmium by cathodic adsorptive stripping voltammetry using artificial neural network. Anal Chim Acta 561:225–232
10. Zheng Y, Huo Q, Kele P, Andreopoulos FM, Pham SM, Leblanc RM (2001) A new fluorescent chemosensor for copper ions based on tripeptide glycyl−histidyl−lysine (GHK). Org Lett 3:3277–3280
11. Zeng L, Miller EW, Pralle A, Isacoff EY, Chang CJ (2006) A selective turn-on fluorescent sensor for imaging copper in living cells. J Am Chem Soc 128:10–11
12. Qi X, Jun EJ, Xu L, Kim S, Hong JSJ, Yoon YJ, Yoon J (2006) New BODIPY derivatives as off-on fluorescent chemosensor and fluorescent chemodosimeter for Cu^{2+}: cooperative selectivity enhancement toward Cu^{2+}. J Org Chem 71:2881–2884
13. Xiang Y, Tong A, Jin P, Ju Y (2006) New fluorescent rhodamine hydrazone chemosensor for Cu(II) with high selectivity and sensitivity. Org Lett 8:2863–2866
14. Yang H, Liu Z, Zhou Z, Shi E, Li F, Du Y, Yi T, Huang C (2006) Highly selective ratiometric fluorescent sensor for Cu(II) with two urea groups. Tetrahedron Lett 47:2911–2914
15. Martinez R, Zapata F, Caballero A, Espinosa A, Tarraga A, Molina P (2006) Rhodamine-diacetic acid conjugate 2-aza-1,3-butadiene derivatives featuring an anthracene or pyrene unit: highly selective colorimetric and fluorescent signaling of Cu^{2+} cation. Org Lett 8:3235–3238
16. Zhang X, Shiraishi Y, Hirai T (2007) Cu(II)-selective green fluorescence of a rhodamine-diacetic acid conjugate. Org Lett 9:5039–5042
17. Li G, Xu Z, Chen C, Huang Z (2008) A highly efficient and selective turn-on fluorescent sensor for Cu^{2+} ion based on calix[4] arene bearing four iminoquinoline subunits on the upper rim. Chem Comm 1774–1776
18. Wu S, Liu S (2009) A new water-soluble fluorescent Cu(II) chemosensor based on tetrapeptide histidyl-glycyl-glycyl-glycine (HGGG). Sens Actuators B 141:187–191
19. Ballesteros E, Moreno D, Gomez T, Rodriguez T, Rojo J, Garcia-Valverde M, Torroba T (2009) A new selective chromogenic and turn-on fluorogenic probe for copper(II) in water-acetonitrile 1:1 solution. Org Lett 11:1269–1272
20. Jung HS, Kwon PS, Lee JW, Kim J, Hong CS, Kim JW, Yan S, Lee JY, Lee JW, Joo T, Kim S (2009) Coumarin-derived Cu^{2+}-selective fluorescence sensor:synthesis, mechanisms, and applications in living cells. J Am Chem Soc 131:2008–2012
21. Zhou Y, Wang F, Kim Y, Kim S, Yoon J (2009) Cu^{2+}-selective ratiometric and "off-on" sensor based on the rhodamine derivative bearing pyrene group. Org Lett 11:4442–4445
22. He G, Zhao X, Zhang X, Fan H, Wu S, Li H, He C, Duan C (2010) A turn-on PET fluorescence sensor for imaging Cu^{2+} in living cells. New J Chem 34:1055–1058
23. Goswami S, Sen D, Das NK (2010) A new highly selective, ratiometric and colorimetric fluorescence sensor for Cu^{2+} with a remarkable red shift in absorption and emission spectra based on internal charge transfer. Org Lett 12:856–859
24. Wu S, Wang T, Liu S (2010) A highly selective turn-on fluorescent sensor for copper(II) ion. Tetrahedron 66:9655–9658
25. Senthilvelan A, Ho I, Chang K, Lee G, Liu Y, Chung W (2009) Cooperative recognition of a copper cation and anion by a calix[4] arene substituted at the lower rim by a ß-amino-a, ß-unsaturated ketone. Chem Eur J 15:6152–6160
26. Benesi HA, Hildebrand JH (1949) A spectrophotometric investigation of the interaction of iodine with aromatic hydrocarbons. J Am Chem Soc 71:2703–2707
27. Singh RB, Mahanta S, Guchhait N (2010) Spectral modulation of charge transfer fluorescence probe encapsulated inside aqueous and non-aqueous β-cyclodextrin nanocavities. J Mol Struc 963:92–97
28. Maeda H, Inoue Y, Ishida H, Mizuno K (2001) UV absorption and fluorescence properties of pyrene derivatives having trimethylsilyl, trimethylgermyl, and trimethylstannyl groups. Chem Lett 1224–1225
29. Karpovich DS, Blanchard GJ (1995) Relating the polarity-dependent fluorescence response of pyrene to vibronic coupling. Achieving a fundamental understanding of the py polarity scale. J Phys Chem 99:3951–3958